Aeroelastic optimisation of manufacturable tow-steered composite wings with cruise shape constraint and gust loads

Aeroelastic optimisation of manufacturable tow-steered composite wings with cruise shape constraint and gust loads

Zhijun Wang, Daniël Peeters, Roeland De Breuker

Faculty of Aerospace Engineering, Delft University of Technology, Kluyverweg 1, 2629 HS Delft, The Netherlands

E-mail: z.wang-16@tudelft.nl

Abstract. In the structural design of aircraft wings, aeroelastic tailoring is used to control the aeroelastic deformation to improve the aerostructural performance by making use of directional stiffness. Recently, tow-steered composites, where the fibre angles continuously vary within each ply, have been proven to have the potential to further expand the advantages of aeroelastic tailoring. This work extends TU Delft aeroelastic tailoring framework PROTEUS by introducing a lay-up retrieval step, so that it can be used for the conceptual design of tow-steered composite wing structures. In the extended framework, aeroelastic tailoring and lay-up retrieval are sequentially and iteratively performed to take static and dynamic loads, manufacturing and cruise shape constraints into consideration. The first step is carried out using PROTEUS, in which the lamination parameters and thickness of the wing sections are optimised under manoeuvre and gust load conditions. Further, for ensuring optimal aircraft performance in cruise flight conditions, the jig twist distribution is allowed to be optimised to maintain a desired prescribed cruise shape. In the second step, the stacking sequence, including minimum steering radius constraint, is retrieved. Since the lamination parameters cannot be matched exactly during the retrieval step, the constraints are checked, and tightened to take the performance loss during retrieval into account. The first step is repeated until all constraints are satisfied after fibre angle retrieval. To demonstrate the usefulness of the proposed optimisation framework, it is applied to the design of the NASA Common Research Model (CRM) wing, of which the objective is minimizing wing mass subjected to aerostructural design constraints, such as aeroelastic stability, aileron effectiveness, material strength and buckling load.

1. Introduction

Composite materials have been widely used in the structural design of aircraft wings, due to their high stiffness-to-mass and strength-to-mass ratios. Further, composites provide the freedom to tailor the wing stiffness in desirable directions, so that the wing deformation can be controlled to introduce the beneficial aeroelastic effects for improving aircraft performance, e.g., wash-out effect. This concept usually is referred to as *aeroelastic tailoring*. Given the manufacturability and certification, in practice, the most common type of composites used for aircraft wings are stacked with $0/\pm45/90$ deg angle unidirectional plies. However, with the advent of automated fiber placement machines, it is possible to efficiently manufacture composite structures with curved fibre trajectories, often referred to as *tow-steered* or *variable stiffness* laminates. In comparison to the conventional straight-fibre laminates, the tow-steered laminates have the

potential to further expand the advantages of aeroelastic tailoring, e.g., increasing the flutter speed [1], because of their larger design space of fibre angles. Therefore, using the tow-steered composites for aeroelastic tailoring of aircraft wings is expected to draw more and more attention in the near future.

To take full advantage of tow-steered composites and aeroelastic tailoring, they have been incorporated into optimisation frameworks for wing aerostructural design. Currently, there are some but limited researches on aeroelastic optimisation of tow-steered composite wings. To name but a few, Stanford and Jutte [2] compared the benefits of aeroelastic tailoring with the use of curvilinear stiffeners and tow-steered composites. They found both methods can reduce the wing mass compared to their non-curvilinear structural counterparts. In another study, Brooks et al. [3] investigated the reduction of fuel burn for tow-steered composite wings using a high-fidelity aerostructural optimisation method. In the existing research work, to the best of the authors' knowledge, only the manoeuvre loads are considered for sizing the tow-steered composite wings except the study of Stodieck et al. [4]. In their work, however, the finite difference method is used to calculate the sensitivities of gust constraints and the jig shape sensitivity was neglected.

This work aims to extend TU Delft aeroelastic tailoring framework PROTEUS by introducing a lay-up retrieval step, so that it can be used for the conceptual design of tow-steered composite wing structures. In comparison to the existing studies, the presented method enables to take gust loads and cruise shape constraints into consideration with full analytic sensitivities provided. Further, the manufacturable fibre paths obtained in this work are retrieved from the optimal distribution of fibre angles, which are not limited to specific patterns. Particularly, a correction strategy is proposed in the present framework for tightening the violated constraints after lay-up retrieval, so that a manufacturable design that satisfies all design constraints can be obtained.

2. Optimisation framework

The aeroelastic optimisation framework proposed for the design of tow-steered composite wings is depicted in Figure 1. It is constructed by sequentially and iteratively performing 1) aeroelastic tailoring and 2) lay-up retrieval. In the first step, the Lamination Parameters (LPs) and thickness of the wing sections are optimised under given loading conditions. Further, for ensuring optimal aircraft performance in cruise flight conditions, the jig twist distribution angles are included as design variables next to LPs and thickness, so that they can be optimised to achieve a desired prescribed cruise shape. The first step is implemented within TU Delft's aeroelastic optimisation tool PROTEUS, which is briefly reviewed in Section 2.1. Subsequently, in the second step, the stacking sequence, including minimum steering radius constraint, is retrieved to match optimal LPs and thickness distribution. Further information on the retrieval step refers to Section 2.2. Since the lamination parameters cannot be matched exactly during the retrieval step, the constraints are checked, and tightened to take the performance loss during retrieval into account. The first step is repeated until all constraints are satisfied after fibre angle retrieval. The strategy applied for tightening the violated constraints is described in Section 2.3. Furthermore, when repeating the aeroelastic tailoring, the aeroelastic and sensitivity analyses of PROTEUS are performed with the updated LPs, thickness and jig twist distribution. Finally, the optimisation process is terminated when all constraints are satisfied after retrieving the manufacturable stacking sequence. In addition, the manufacturable fibre paths are obtained by post-processing the retrieved fibre angle distributions.

2.1. Aeroelastic tailoring in PROTEUS

In the optimisation framework depicted in Figure 1, the aeroelastic tailoring of a wing is carried out using a tool, PROTEUS, developed at TU Delft. In PROTEUS, the wing geometry is divided into a number of sections with an independent laminate distribution assigned to each section. The stiffness properties of wing laminates are parameterized by lamination parameters,

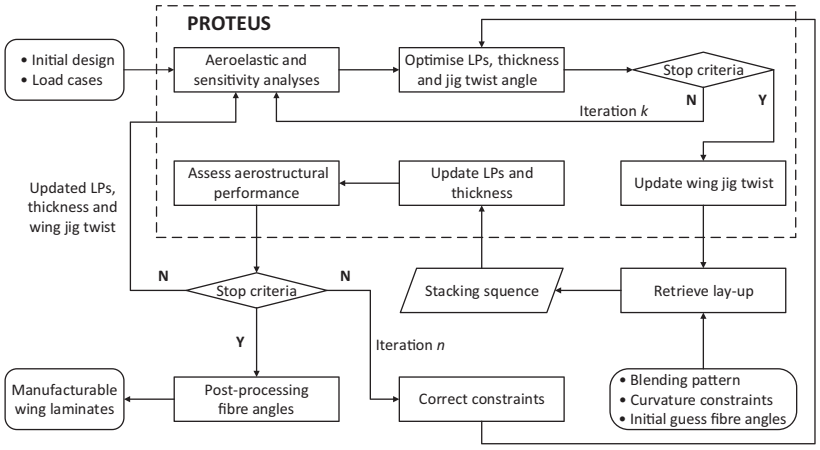

Figure 1. Flowchart of the aeroelastic optimisation framework for the design of tow-steered composite wings, with iterations k and n referring to inner and outer loops, respectively.

which provides a continuous design space for the use of gradient-based optimisation methods. For efficiency, the 3D wing is modelled as a 1D beam using a geometrically nonlinear beam finite element model, where the cross-sectional stiffness matrix of each section is determined using a cross-sectional modeller. The cross-sectional modeller discretizes the cross-section using linear Hermitian shell elements, then the cross-sectional stiffness matrix is determined using a variational asymptotic method. Further details about the cross-sectional modeller refer to the work of Ferede and Abdalla [5]. This cross-sectional modeller is also used for recovering the strain in each cross-section when the aeroelastic analysis has been completed. Regarding to aeroelastic analysis, PROTEUS is able to predict both the static and dynamic aeroelastic responses. The static aeroelastic model closely couples the nonlinear beam model and a steady aerodynamic model that is constructed using vortex lattice method based on potential flow theory. The nonlinear stiffness matrix, obtained using the static aeroelastic model, is linearised around the static equilibrium position and coupled to a linear mass matrix for obtaining a dynamic structural model. Then this structural model is coupled to an unsteady aerodynamic model to construct the dynamic aeroelastic model that allows for analysing the aeroelastic response of the wing under gust loads. More details on the PROTEUS refer to the work of Werter and De Breuker [6]. In the present work, optimising the jig twist distribution is realised by making use of the morphing function of PROTEUS [7].

2.2. Lay-up retrieval optimisation

In aeroelastic tailoring, PROTEUS determines the optimal LPs and thickness of wing laminates, which then requires an additional lay-up retrieval step to obtain the laminate stacking sequence. In this work, a method to optimise manufacturable fibre angle distributions of tow-steered laminates [8] is employed to retrieve the stacking sequence of wing laminates. This approach starts from a discretisation of the composite structure into a shell finite element model (not to be confused with the beam element model introduced in Section 2.1 because the aeroelastic tailoring and fibre angle retrieval are carried out using different tools) whereby the fibre angles are defined at the element nodes. Accordingly, the optimal fibre angle distribution over the structure can be determined by solving an optimisation problem which aims to match the optimal LPs obtained from aeroelastic tailoring. Particularly, a minimum steering radius constraint, defined as the rate of change in fibre angle between nodes, is introduced in the optimisation to ensure the laminate can be manufactured using automated fibre placement machines and avoid fibre wrinkling caused

by a too small steering radius. Additionally, the laminate thickness obtained from aeroelastic tailoring is rounded up to the nearest number of plies in the lay-up retrieval step. A detailed description on this optimisation method refers to the work of Peeters et al. [8, 9]. According to the optimal fibre angles, the final fibre paths can be obtained using a post-processing procedure presented in the paper of Blom et al. [10].

2.3. Constraint correction strategy

In the framework illustrated in Figure 1, if the constraints are violated after retrieving the manufacturable stacking sequence, then the aeroelastic tailoring step (PROTEUS) is required to be repeated with corrected optimisation constraints. The correction strategy applied for violated constraints is to tighten the original constraint value by the percentage linked to the constraint violation, so that the loss in performance during the retrieval step can be taken into account while repeating aeroelastic tailoring. The constraint value used in PROTEUS can be obtained by

$$C_n^i = \begin{cases} v_{n-1}^i C_0^i & \text{if } v_{n-1}^i > s^i\,, \\ s^i C_0^i & \text{otherwise}\,, \end{cases} \quad \text{with} \;\; n > 1, \tag{1}$$

where n is the iteration number of performing PROTEUS (as indicated in Figure 1) and i is the index of the design constraint. Accordingly, C_n^i represents the value of the i-th constraint at the n-th time of performing PROTEUS, and C_0^i is the prescribed original value of the i-th constraint. v refers to a violation factor defined as $v_{n-1}^i = c_{n-1}^i / C_0^i$ with $n > 1$, where c is the constraint value calculated from the assessment of aerostructural performance with retrieved stacking sequence. s is a prescribed threshold value for violation factor v, which is introduced to tighten the original constraint value C_0 if the violation factor v is lower than a certain value. At the first time of running PROTEUS (i.e., $n = 1$), the original constraint value C_0^i is used for aeroelastic tailoring. When repeating PROTEUS (i.e., $n > 1$), the constraint value C_n^i is obtained by scaling the original constraint value C_0^i using the violation factor v_{n-1}^i or the threshold value s^i. In the present work, the threshold value $s^i = 1.2$ is defined for every constraint, which means the original constraint value C_0^i need to be tightened 20% for repeating PROTEUS. In general, the larger the predefined threshold value, the less iterations are required, but that may overshadow the gain in aeroelastic tailoring.

3. Numerical examples

3.1. Optimisation setup

To demonstrate the usefulness of the proposed optimisation framework, it is applied to the design of the NASA CRM wing. The details on modelling CRM wing within PROTEUS framework refer to the work of Macquart et al. [11], Rajpal et al. [12] and references therein. In the current work, three static and one dynamic load cases, listed in Table 1, are considered for wing design. The static load cases represent the cruise condition, 2.5 g symmetric pull up and -1 g symmetric push down manoeuvres, respectively. For the dynamic load case, the wing model is subjected to a discrete 1-cosine gust given by EASA CS-25 regulations [13], and four critical gust lengths, 50, 70, 90 and 110 m, are selected to be evaluated during the optimisation process.

The optimisation aims to minimize the wing mass subjected to the design constraints listed in Table 2. Note that the wing mass is normalised by that of initial design and the constraint on minimum steering radius is applied in the lay-up retrieval step. Further, Table 2 only lists the type of optimisation constraints, the actual number of constraints also depends on the amount of section and load case of the wing. Table 3 gives the material properties used for CRM wing design. For simplicity, only the top and bottom skins of the wing are treated as design domain,

Table 1. Load cases defined for the aeroelastic optimisation of the CRM wing.

ID	Description	V_{EAS} (m/s)	Altitude (m)	Mach	Load factor	Fuel level (Tank 1-4)			
1	Cruise	136	11000	0.85	1.0	0.7	0.7	0.7	0.7
2	Symm. pull up	240	3000	0.85	2.5	0.8	0.8	0.8	0.8
3	Symm. push down	198	0	0.60	-1.0	0.8	0.8	0.8	0.8
4	Dynamic gust*	140	0	0.41	1.0	0.8	0.8	0.8	0.8

* Gust length: 50, 70, 90 and 110 m.

the LPs and thickness of wing spars are predefined and fixed in optimisation. Moreover, each wing skin is divided into 10×2 (spanwise $\times$ chordwise) sections.

Table 2. Optimisation objective, design variables and constraints for the design of the CRM wing.

Objective	Minimum wing mass
Design variables	LPs and thickness Jig twist distribution angles
Constraints	Lamination parameter feasibility Aeroelastic stability Local angle of attack Aileron control effectiveness Tsai-Wu strain factor Buckling factor Cruise twist distribution Steering radius (curvature)

Table 3. Material properties of AS4/3501-6.

Property	Value
E_{11}	147.0 GPa
E_{22}	10.3 GPa
G_{12}	7.0 GPa
ν_{12}	0.27 GPa
ρ	1600 kg/m^3
X_t	984.5 MPa
X_c	717.6 MPa
Y_t	23.7 MPa
Y_c	94.8 MPa
S	31.6 MPa

In order to investigate the effects of cruise shape constraint and gust loads on wing structural design, three case studies with different loading conditions and optimisation constraints are defined and carried out. In both *Cases 1* and *2*, only the static loads listed in Table 1 are considered, but the cruise twist constraint and the jig twist distribution design variables are included in *Case 2*, while *Case 3* is defined to consider also gust loads based on *Case 2*.

3.2. Results and discussion

Figure 2 illustrates the convergence behaviour of the normalised wing mass and the number of violated constraints for *Case 1*. It can be observed that 16 constraints (including 15 strain factor and 1 aileron control effectiveness of Load case 2) are violated after the first retrieval step. At the second time of running PROTEUS (i.e., $n = 2$), the mass reduction gained from previous iteration ($n = 1$) is decreased in order to satisfy the tighter constraints. In the present work, all three case studies require only two iterations for the outer loop ($n = 2$) to reach a converged solution.

The cruise (1 g) and jig (unloaded) twist distribution of the optimised wing for *Cases 1, 2* and *3* are plotted in Figure 3. Comparing the 1 g twist distribution obtained in *Case 1* with the desired prescribed target, a significant difference can be observed because the cruise twist

constraint is not taken into account in *Case 1*. However, in both *Cases 2* and *3*, the 1 g twist distribution of the optimised wing has a good agreement with the target as a result of including the cruise twist constraint. Accordingly, the jig twist distribution of the wing has been changed in both *Cases 2* and *3* to satisfy the constraint on cruise twist distribution. Additionally, note that the wings obtained in all cases seem to be stiff because the aileron control effectiveness constraint is active to size the wing tip regions. It is expected to have a more flexible wing when the constraint on aileron control effectiveness is removed from optimisation.

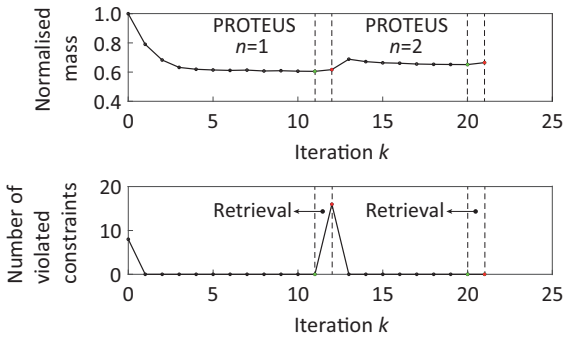

Figure 2. Convergence behaviour of the normalised wing mass and the number of violated constraints for *Case 1*.

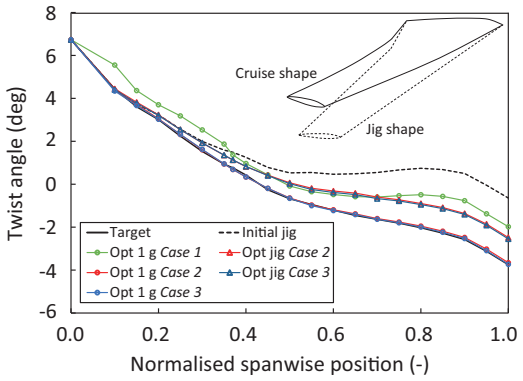

Figure 3. Cruise and jig twist distribution of the CRM wing for *Cases 1, 2* and *3*. The inset schematically illustrates the jig and cruise shape of a wing.

Figure 4 shows the thickness distribution of the optimised wing skins for *Cases 1, 2* and *3*. It can be seen that the wings tailored in all three cases have a similar trend in thickness distribution. Namely, the patches at the leading edge are thicker than those at the trailing edge from wing root up to middle span, which introduces the beneficial wash-out effect for reducing wing mass. Conversely, the patches at the trailing edge are thicker than those at the leading edge at the wing tip where the aileron control effectiveness is active for wing sizing. Comparing the normalised wing mass optimised in *Case 2* with that obtained in *Case 1*, it is observed that including the cruise shape constraint and jig twist optimisation results in a mass reduction of 8.9%. The strain factor of the wing in *Case 2* is shown in Figure 5. As can be observed, the wing sized with only static loads (Load cases 1-3) shows failure under gust loads (Load case 4), i.e., strain constraint violation. This demonstrates the importance of including gust loads for a safe wing design. Note that the strain factor plotted in Figure 5 represents the strength failure indicator that is determined by mapping the Tsai-Wu failure criterion onto strain space (details refer to [14]), which explains the discontinuity in the distribution observed in Figure 5.

Accordingly, the wing sized with gust loads (*Case 3*) does not show failure as indicated in Figure 5(b), but its mass is about 15.4% larger than the wing obtained in *Case 2*. Additionally, Figure 6 shows the fiber paths of layer 1 of the optimised wing for *Cases 1, 2* and *3*. Note that these fibre paths are given just as examples, the stiffness distribution of the optimised wing skins cannot be interpreted from Figure 6. Accordingly, Figure 7 shows a comparison of the out-of-plane stiffness distributions of the wing top skin obtained before (colored blue) and after (colored red) retrieving the manufacturable stacking sequence. Here the stiffness distribution is represented using a polar plot of the thickness-normalised modulus of elasticity that is defined as $\hat{E}_{11}(\theta) = 1/\hat{D}_{11}^{-1}(\theta)$ for each laminate, where $\hat{D}$ is the thickness-normalized flexural stiffness matrix and θ ranges from 0 to 360 degrees [15]. It can be observed that the stiffness distributions obtained before and after retrieval differ at the first iteration $k = 1$, which causes the constraint

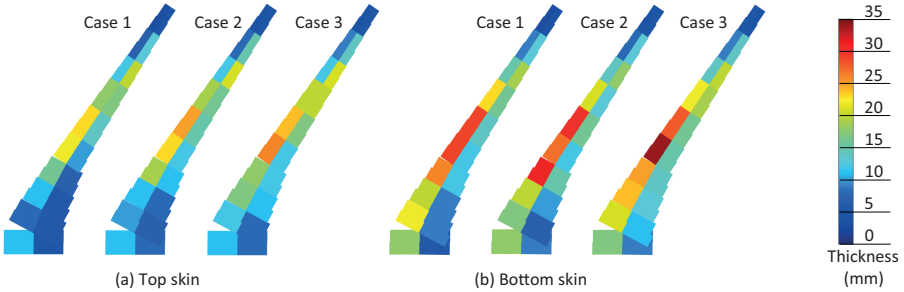

Figure 4. Thickness distribution of the optimised wing skins for *Cases 1, 2* and *3*.

violations and necessitates the second iteration $k = 2$ with tighter constraints. It is clear that the wing stiffness distributions obtained before and after retrieval show good agreement when reaching a converged solution (i.e., iteration $k = 2$), which demonstrates the validity of the proposed optimisation framework.

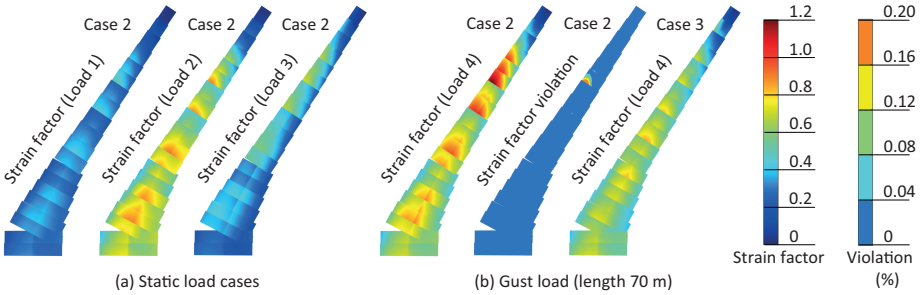

Figure 5. Strain factor of the wing optimised without and with gust loads.

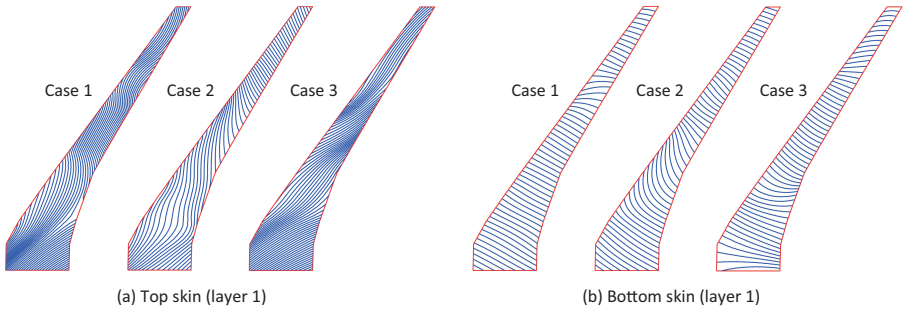

Figure 6. An example of fibre paths (layer 1) of the optimised wing for *Cases 1, 2* and *3*.

4. Conclusions

In the current work, the aeroelastic tailoring framework PROTEUS has been extended for the conceptual design of tow-steered composite wings, which enables to take manoeuvre and gust loads, manufacturing and cruise shape constraints into consideration. The framework is extended by sequentially and iteratively performing aeroelastic tailoring and lay-up retrieval. During aeroelastic tailoring, the lamination parameters and thickness of wing laminates are optimised for reducing wing mass subjected to aerostructural design constraints, such as aeroelastic stability,

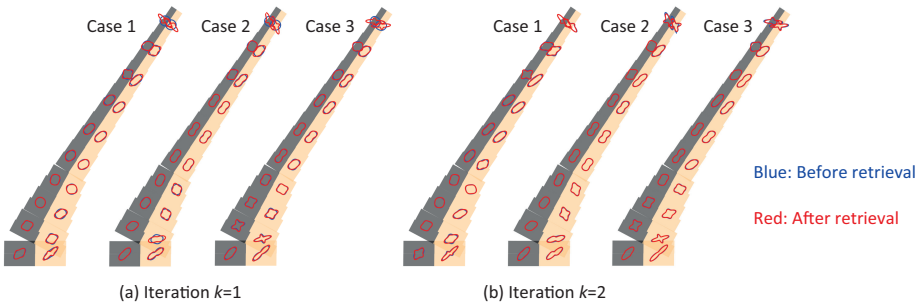

Figure 7. Out-of-plane stiffness distributions of the wing top skin obtained before and after the first and second time of retrieving the stacking sequence for *Cases 1, 2* and *3*.

aileron effectiveness, material strength and buckling load. Further, the jig twist distribution of the wing is optimised to maintain a desired prescribed cruise shape. In lay-up retrieval, the manufacturable stacking sequence is retrieved by including minimum steering radius constraint. To address the violated constraints after lay-up retrieval, a correction strategy has been proposed for tightening the violated constraints, so that the loss in performance during the retrieval step can be taken into account while repeating aeroelastic tailoring.

To demonstrate the usefulness of the proposed optimisation framework, it has been applied to the design of the NASA CRM wing, whereby the effects of cruise shape constraint and gust loads on aeroelastic tailoring of the wing have been investigated. The optimisation results show that the wing mass can be further reduced by including the cruise shape constraint and jig twist optimisation. Further, the wing sized with only static loads may show failure under gust loads, while the wing optimised with gust loads results in an increased mass compared to the statically tailored wing. Therefore, it is important to consider gust loads and cruise shape constraint for the design of aircraft wings, which demonstrates the importance and usefulness of the proposed optimisation framework.

Acknowledgments

This work is supported by the AGILE 4.0 project (Towards Cyber-physical Collaborative Aircraft Development) and has received funding from the European Union's Horizon 2020 Programme under grant agreement n^{o} 815122.

References

[1] Stodieck O, Cooper J E, Weaver P M and Kealy P 2013 *Composite Structures* **106** 703–715
[2] Stanford B K and Jutte C V 2017 *Computers & Structures* **183** 48–60
[3] Brooks T R, Martins J R R A and Kennedy G J 2019 *Journal of Fluids and Structures* **88** 122–147
[4] Stodieck O, Cooper J E, Weaver P M and Kealy P 2017 *AIAA Journal* 1425–1439
[5] Ferede E A and Abdalla M M 2014 *55th AIAA/ASME/ASCE/AHS/ASC Structures, Structural Dynamics, and Materials Conference* p 0163
[6] Werter N and De Breuker R 2016 *Composite Structures* **158** 369–386
[7] De Breuker R, Abdalla M M and Gürdal Z 2011 *Journal of Intelligent Material Systems and Structures* **22** 1025–1039
[8] Peeters D M, Hesse S and Abdalla M M 2015 *Composite Structures* **125** 596–604
[9] Peeters D M, Lozano G G and Abdalla M M 2018 *Computers & Structures* **196** 94–111
[10] Blom A W, Abdalla M M and Gürdal Z 2010 *Composites Science and Technology* **70** 564–570
[11] Macquart T, Werter N and De Breuker R 2017 *Journal of Aircraft* **54** 561–571
[12] Rajpal D, Kassapoglou C and De Breuker R 2019 *Composite Structures* **227** 111248
[13] EASA 2020 *Amendment* **25**
[14] Khani A, IJsselmuiden S T, Abdalla M M and Gürdal Z 2011 *Composites Part B: Engineering* **42** 546–552
[15] Dillinger J K S, Klimmek T, Abdalla M M and Gürdal Z 2013 *Journal of Aircraft* **50** 1159–1168